

# Molecular pathophysiology of mucopolidosis type IV: pH dysregulation of the mucolipin-1 cation channel

Malay K. Raychowdhury<sup>1,2,†</sup>, Silvia González-Perrett<sup>3,4,†</sup>, Nicolás Montalbetti<sup>3</sup>, Gustavo A. Timpanaro<sup>3</sup>, Bernard Chasan<sup>5</sup>, Wolfgang H. Goldmann<sup>1,2</sup>, Stefanie Stahl<sup>6</sup>, Adele Cooney<sup>6</sup>, Ehud Goldin<sup>6</sup> and Horacio F. Cantiello<sup>1,2,3,\*</sup>

<sup>1</sup>Renal Unit, Massachusetts General Hospital East, Charlestown, MA, USA, <sup>2</sup>Department of Medicine, Harvard Medical School, Boston, MA, USA, <sup>3</sup>Laboratorio de Canales Iónicos, Departamento de Físicoquímica y Química Analítica, Facultad de Farmacia y Bioquímica, Buenos Aires, Argentina, <sup>4</sup>Departamento de Fisiología, Facultad de Medicina, Buenos Aires, Argentina, <sup>5</sup>Physics Department, Boston University, Boston, MA, USA and <sup>6</sup>Developmental and Metabolic Neurology Branch, National Institutes of Health, Bethesda, MD, USA

Received October 28, 2003; Revised January 12, 2004; Accepted January 25, 2004

**Mucopolidosis type IV (MLIV) is an autosomal recessive neurogenetic disorder characterized by developmental abnormalities of the brain and impaired neurological, ophthalmologic and gastric function. Large vacuoles accumulate in various types of cells in MLIV patients. However, the pathophysiology of the disease at the cellular level is still unknown. MLIV is caused by mutations in a recently described gene, *MCOLN1*, encoding mucolipin-1 (ML1), a 65 kDa protein whose function is also unknown. ML1 shows sequence homology and topological similarities with polycystin-2 and other transient receptor potential (Trp) channels. In this study, we assessed both, whether ML1 has ion channel properties, and whether disease-causing mutations in *MCOLN1* have functional differences with the wild-type (WT) protein. ML1 channel function was assessed from endosomal vesicles of null (*MCOLN1*<sup>-/-</sup>) and ML1 over-expressing cells, and liposomes containing the *in vitro* translated protein. Evidence from both preparations indicated that WT ML1 is a multiple subconductance non-selective cation channel whose function is inhibited by a reduction of pH. The V446L and ΔF408 MLIV causing mutations retain channel function but not the sharp inhibition by lowering pH. Atomic force imaging of ML1 channels indicated that changes in pH modified the aggregation of unitary channels. Mutant-ML1 did not change in size on reduction of pH. The data indicate that ML1 channel activity is regulated by a pH-dependent mechanism that is deficient in some MLIV causing mutations of the gene. The evidence also supports a novel role for cation channels in the acidification and normal endosomal function.**

## INTRODUCTION

Mucopolidosis type IV (MLIV) is a rare genetic disorder originally described by Berman *et al.* in 1974 (1). Clinically diagnosed by psychomotor retardation and altered degree of visual impairment within the first year of life (2), most MLIV affected individuals are unable to speak and walk. MLIV patients also have abnormalities in white matter (3), indicative of a developmental brain disorder. Atrophic changes in the cerebellum and the optic nerve are examples of progressive deteriora-

tion in MLIV. MLIV patients show abnormal vacuoles, which stain with lysosomal markers (4). The vacuoles are more prominent in secretory epithelial cells such as corneal epithelial (5), pancreas acinar (6) and stomach parietal cells (7). Parietal cells also manifest the only MLIV-specific known biochemical abnormality, achlorhydria, associated with an elevated gastrin secretion (8).

MLIV is caused by mutations in the recently discovered *MCOLN1* gene, encoding a novel protein, mucolipin-1 (ML1) (9,10). *MCOLN1* mutations have been identified predominantly

\*To whom correspondence should be addressed at: Renal Unit, Massachusetts General Hospital East, 149 13th Street, Charlestown, MA 02129, USA. Tel: +1 6177265640; Fax: +1 6177265669; Email: cantiello@helix.mgh.harvard.edu

<sup>†</sup>The authors wish it to be known that, in their opinion, the first two authors should be regarded as joint First Authors.

in Ashkenazi Jewish (AJ), but also non-jewish (NJ) patients (11). Two founder MCOLN1 mutations were identified comprising 95% of mutant alleles in Ashkenazi MLIV families (9,10,12), in correlation with two haplotypes in the chromosomal region (13). The most common AJ mutations result in a null-expression based on the prediction of the defect in MCOLN1 mRNA and northern blots (10). Other mutations that only cause a minor change in the predicted sequence of ML1 result in a variety of phenotypes. These range from the F408 deletion ( $\Delta$ F408), an in-frame amino acid deletion identified in a patient with an unusually mild case of the disease to more severe phenotypes (2). Two patients have been reported (2), with an intermediate form of MLIV, based on consecutive amino acid substitutions, namely V446L and L447P, in the expected fifth transmembrane (TM) of the protein (see below). These MLIV causing mutations are expected to have ML1 activity as is reported in the present study. To date, there is no clear functional correlation between the various mutations and the differences in the phenotypic severity of MLIV. This study attempts to correlate different functional aspects of ML1 with MLIV causing mutations.

ML1 is a 580 amino acid long protein (~65 kDa). Comparison of ML1 with known protein motifs and patterns of ProfileScan identified a transient receptor potential (Trp) channel-related region (PS50272, aa 331–521) and an internal  $\text{Ca}^{2+}$  and  $\text{Na}^{+}$  channel pore region (aa 496–521). As a Trp-type channel, the topology follows that expected six putative TM domains, and both N- and carboxy terminal ends facing the same side of the membrane (10). The Trp-similar region spans TM segments 3–6, with a putative pore-forming (P) loop between TMs 5 and 6. ML1 also contains two Pro-rich regions (aa 28–36 and 197–205), a lipase serine active site domain (aa 104–114). A di-leucine motif (L-L-X-X) motif present at the carboxy-terminal end of ML1 may be suggestive of late endosomal/lysosomal targeting. Strong sequence identity (38%) is observed between ML1 and a putative *Drosophila* ortholog gene, with nearly perfect conservation of the Trp channel and pore region domains (58% identity). ML1 also has strong topological homology with the polycystin-2 channel (10). At least one recent report has implicated ML1 expression with cation-selective channel activity (14). In that study, expression of the full-length MCOL1 cDNA into *Xenopus* oocytes was associated with the presence of a novel channel with a large conductance and permeability to  $\text{Na}^{+}$ ,  $\text{K}^{+}$  and  $\text{Ca}^{2+}$ . In the present study, we show that ML1 is a pH-dependent cation channel, whose dysfunction is likely associated with the genesis of MLIV.

## RESULTS

### Cation channel activity of ML1-containing endosomes

Endosomal vesicles containing wild-type (WT) ML1 were reconstituted in a lipid bilayer system to assess for channel activity (Fig. 1). Spontaneous cation channel activity was observed in the presence of 150 mM  $\text{K}^{+}$  in the *cis*-side and 15 mM  $\text{K}^{+}$  in the *trans*-side of the reconstitution chamber (Fig. 1A,  $n=24$ ). A 130–150 pS [ $1 \text{ pS} = 10^{-12} \text{ S}$  (Siemens) where  $1 \text{ S} = 1 \text{ Ampere/Volt}$ ] single channel conductance was

observed (Fig. 1B,  $n=3$ ), which was absent in endosomes from *MCOLN1*<sup>-/-</sup> cells (data not shown). Large conductance channels often ‘disorganized’ into smaller channel levels (Fig. 1C, left), consistent with multi-channel complexes. Sub-conductance states included a frequent 35 pS channel level (Fig. 1B,  $n=8$ ). Channel activity was also found in endosomes expressing  $\Delta$ F408-, but not D362Y-ML1 (Table 1). While  $\Delta$ F408-ML1 produces the mildest known case of the disease, D362Y-ML1 is known for an intermediate disease, known in two cases (2). The smaller ML1 single channel conductances were obtained by noise (mean versus variance) analysis (15,16) (Fig. 1C, right  $n=5$ ). The data sorted into at least three conductance states, the smaller one of which was 5 pS (only disclosed by mean versus variance analysis). The ML1 multi-channel behavior was more clearly observed by channel inhibition elicited by lowering  $\text{pH}_{\text{cis}}$  (Fig. 1D). A decrease of pH from 7.4 to 6.4 inhibited the mean current by 61.4% ( $26.6 \pm 4.42$  versus  $10.2 \pm 3.19 \text{ pA}$ ,  $n=6$ ,  $P < 0.01$ ). The pH inhibited endosomal channel activity re-activated upon addition of KOH (Fig. 1D,  $n=4$ ).

### Channel activity of *in vitro* transcribed/translated mucolipin-1

To confirm WT-ML1 cation channel activity, the expression vector containing the entire sequence for the WT-human ML1 was *in vitro* transcribed and translated, and dialyzed into liposomes. Two mutant ML1, V446L-ML1 and  $\Delta$ F408-ML1 were also prepared and compared in size and purity with the WT translated product by SDS-PAGE. WT-ML1 containing liposomes were reconstituted in a lipid bilayer system, in a  $\text{K}^{+}$  gradient. Spontaneous, cation-selective single channel currents (Fig. 2A and B) were observed, with a most frequent single channel conductance of  $46.3 \pm 9.44 \text{ pS}$  (Fig. 2B,  $n=3$ ). This conductance varied among preparations, suggesting channel complexes composed of various channel numbers. Single channel recordings showed multiple substate levels (Fig. 2C). Mean versus variance analysis (Fig. 2D) unmasked a main conductance of 35.8 pS, and 5.52 and 1.02 pS smaller single channel conductances. The fraction of time the channel remains open, (open probability,  $p_o$ ) in the most frequent open channel level, was strongly voltage dependent and decreased at negative potentials (Fig. 2E). This was characterized by fitting the  $p_o$  versus  $V_m$  data with the Boltzmann equation (17), which rendered the following parameters,  $p_{\text{max}} = 0.83 \pm 0.10$  ( $n=3$ ),  $k = 36.2 \pm 22$ , and  $V_m = -29.0 \pm 19 \text{ mV}$ . The *in vitro* translated WT-ML1 channel permeated both  $\text{Na}^{+}$  and  $\text{Ca}^{2+}$  with frequent bursts of channel inactivation (data not shown). WT-ML1 was inhibited (84%,  $n=7$ ) with amiloride (1 mM, Fig. 2F). Two disease-causing mutants of ML1, V446L and  $\Delta$ F408 were also tested for ion channel function. Both ML1 mutants displayed spontaneous cation channel activity (Fig. 2G) in asymmetrical  $\text{K}^{+}$ , and  $\text{K}^{+}/\text{Na}^{+}$  gradients. A single channel conductance of  $27.0 \pm 1.21 \text{ pS}$  ( $n=4$ ) was observed for  $\Delta$ F408-ML1 (Fig. 2H, top), and  $42.2 \text{ pS}$  ( $n=1$ ) for V446L-ML1 (Fig. 2H, top). Mean versus variance analysis (Fig. 2H, bottom) disclosed smaller single channel conductances of  $1.58 \pm 0.08 \text{ pS}$  ( $n=3$ ) and  $1.79 \pm 0.11 \text{ pS}$  ( $n=3$ ) for  $\Delta$ F408-ML1 and V446L-ML1, respectively. Conductances of 6.03 pS ( $n=3$ ) and 5.02 pS

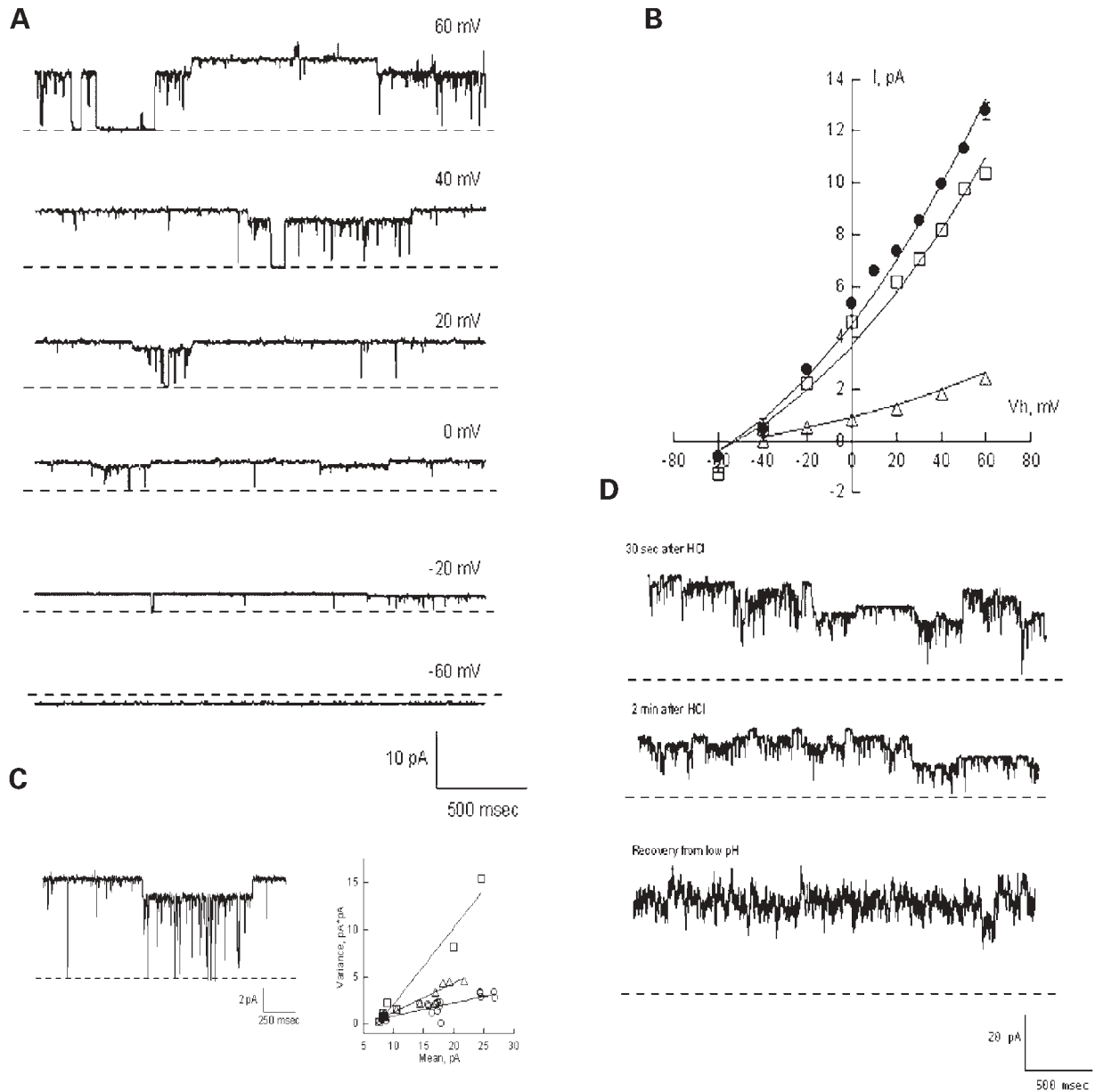


**Figure 1.** Functional characterization of ML1-containing endosomal channels. (A) WT-ML1-containing endosomes were reconstituted in a lipid bilayer system. Spontaneous cation channel activity was observed in either  $\text{Cl}^-$  or gluconate containing  $\text{K}^+$  salts. Data are representative of 24 experiments. (B) Current-to-voltage relationship of most common single channel conductances in asymmetrical  $\text{K}^+$ . Solid lines represent GHK fitting of experimental data. The chord conductances were 150 pS (filled circles), 135 pS (open squares) and 35 pS (open triangles), respectively ( $n = 3$ ). The reversal potential ( $-52 \text{ mV}$ ), indicates a high cation/anion perm-selectivity ratio. (C) Left: large single channel currents were the composite of multiple subconductance states, one of which is shown in the tracing (data representative of 5). Right: mean versus variance analysis identified three conductances (linear regression lines). Holding potential was 40 mV. Three common levels were identified, with conductances shown by linear regression lines. (D) WT-ML1 channel activity decreased after addition of HCl (top two tracings), unmasking various single channel current levels. Addition of KOH (lower tracing) to the *cis* side of the reconstitution chamber reversed the inhibitory effect on channel activity. Data are representative of three experiments. Holding potential was 40 mV.

( $n = 3$ ) for the  $\Delta\text{F408}$  and the V446L mutants, respectively, were also obtained by mean versus variance analysis. This is a correlation between the mean and the variance of the currents tracings at a given potential [for theory, see (18)]. Thus, the small unitary conductance was similar in both WT- and mutant-ML1. In contrast to WT-ML1, V446L ML1 often showed currents at negative potentials (Fig. 2H, top) and a shift in the

Boltzmann response to voltage (data not shown). Mutant-ML1 was also inhibited by amiloride (Fig. 2G, bottom tracing).

#### Effect of pH on ML1 cation channel activity

To assess a potential molecular mechanism for the genesis of MLIV, and confirm the data with ML1-containing endosomes,

**Table 1.** Comparison of wild-type and mutated ML1 channels from various preparations

ML1 Type	Channel function	Preparation	Conductance		pH sensitive
			Current analysis (pS)	Mean versus variance analysis (pS)	
Wild	Yes	Endosome	35 <sup>a</sup>	5	Yes
	Yes	<i>in vitro</i>	46 <sup>b</sup>	36/6	Yes
V446L	Yes	<i>in vitro</i>	12/2.6	37/5.6	No
ΔF408	Yes	Endosome	49/15/6	70/6.7	No
	Yes	<i>in vitro</i>	27	6	No
D362Y	No	Endosome	—	—	—

<sup>a</sup>Also 130–150 pS in endosomes, where channels seemed to behave in highly organized clusters.

<sup>b</sup>Value has a large dispersion, indicating various complexes (see text).

the effect of pH on WT-ML1 was determined (Fig. 3A). WT-ML1 channel activity was completely blocked after decreasing  $pH_{cis}$  (Fig. 3A). This effect was partially reversible, upon addition of KOH to restore normal pH (Fig. 3A). Changes in pH did not modify the small, single-channel conductance of the WT-ML1 channel, as determined by mean versus variance analysis (Fig. 3B). WT-ML1 cation channel activity exponentially decreased as a function of decreasing  $pH_{cis}$  (Fig. 3C). At pH 6.0, channel activity was, on average, 82% lower than control currents (pH 7.15). Fitting the experimental data to a Henderson–Hasselbach type of pH equation (19) indicated an apparent  $pK_a$  of 6.66 (Fig. 3C). Reduction of  $pH_{cis}$  (~5.0), however, had no significant effect on the mean channel activity of either mutant-ML1 (Fig. 3D). Low  $pH_{cis}$  reduced ΔF408 ML1 channel activity by 39% ( $P < 0.2$ ), while V446L-ML1 currents increased by 110% ( $P < 0.1$ ). Neither change was statistically different with respect to its own control value (Fig. 3D). The data are most consistent with a dysfunctional response of the mutant-ML1 channels to low pH.

#### Atomic force microscopy (AFM) of mucolipin-1 channel clusters

ML1 channel activity indicated complexing of single channel clusters. Thus, pH changes may play a role in ML1 channel assembly as postulated for other channel (20–22) and receptor (23) preparations. To test whether pH modulates channel clustering, WT- and mutant-ML1 (Fig. 4) were flattened onto freshly cleaved mica and scanned by AFM in saline solution, as we have recently reported for another channel (24). WT-ML1 complexes (Fig. 4A, left) changed in size at low pH (Fig. 4A, right). The size of the molecular complexes was obtained from horizontal scan lines (Fig. 4B). Height versus diameter distributions for complexes at normal and low pH (Fig. 4C) indicated a change in diameter (Fig. 4D). At least four peaks in diameter were observed at normal pH, which decreased to two at low pH, indicating a change in the diameter of the molecular complex. The height of the ML1 channel complexes also decreased by 28% after low pH ( $0.89 \pm 0.08$ ,  $n = 40$  versus  $0.64 \pm 0.07$ ,  $n = 37$ , respectively,  $P < 0.01$ ). Thus, spontaneous aggregation of WT-ML1 complexes at normal pH (7.15, Fig. 4E), decreased at low pH (Fig. 4E). A pH change of V446L-ML1 (Fig. 4E) and ΔF408-ML1 (Fig. 4E), however, showed lower disassembly. This is in agreement with the

contention that lowering pH fails to modify the size of mutated ML1 channel complexes.

## DISCUSSION

The data in this report demonstrate that WT-ML1 is a cation channel, whose regulation by pH is missing in two MLIV-causing mutations that retain ML1 channel function. ML1 channel function was assessed in endosomal vesicles of null (*MCOLN1*<sup>-/-</sup>) and ML1 over-expressing cells. Only the ML1-containing endosomes showed cation channel activity, consistent with over-expression of the protein. Channel activity by ML1 was confirmed by reconstitution of the *in vitro* translated protein. Evidence from both preparations indicated that the WT-ML1 channel conductance is composed of multiple subconductance states of the channel, whose function is inhibited by a reduction of pH. The V446L and ΔF408 MLIV causing mutations retain channel function of ML1, but not the sharp inhibition by lowering pH. Based on the multiple subconductance states of the single channel currents, the possibility was explored that the channels are multimeric complexes with various degrees of functional activity. Atomic force imaging of WT-ML1 channel complexes indicated that changes in pH modified the state of aggregation of the unitary channels. Whether this correlates functionally with each monomeric unit of the channel complex will require further investigation. Mutant-ML1 channel complexes did not change in size on reduction of pH, which is in agreement with the lack of effect of the mutant channels to low pH. Thus, the data indicate that a dysfunctional ML1 channel activity by a pH-dependent mechanism may be deficient in some functional MLIV causing mutations of the gene. However, the major MLIV causing mutations are expected to produce no protein (2), suggesting no contribution of the ML1 channel to cell function in the disease.

Three mucolipin genes have been found in humans, and other vertebrates, and only one in invertebrates, e.g. *Drosophila melanogaster* (CG8743) and *Caenorhabditis elegans* (CUP-5) (25,26). The role(s) of the gene products is largely unknown to date, but information is mounting on similar roles in endocytic vesicle trafficking. MLIV is a lipid storage disease, where the traffic of late endocytic/lysosomal vesicle transport is impaired (25,27–29). This is consistent with the fact that the absence of

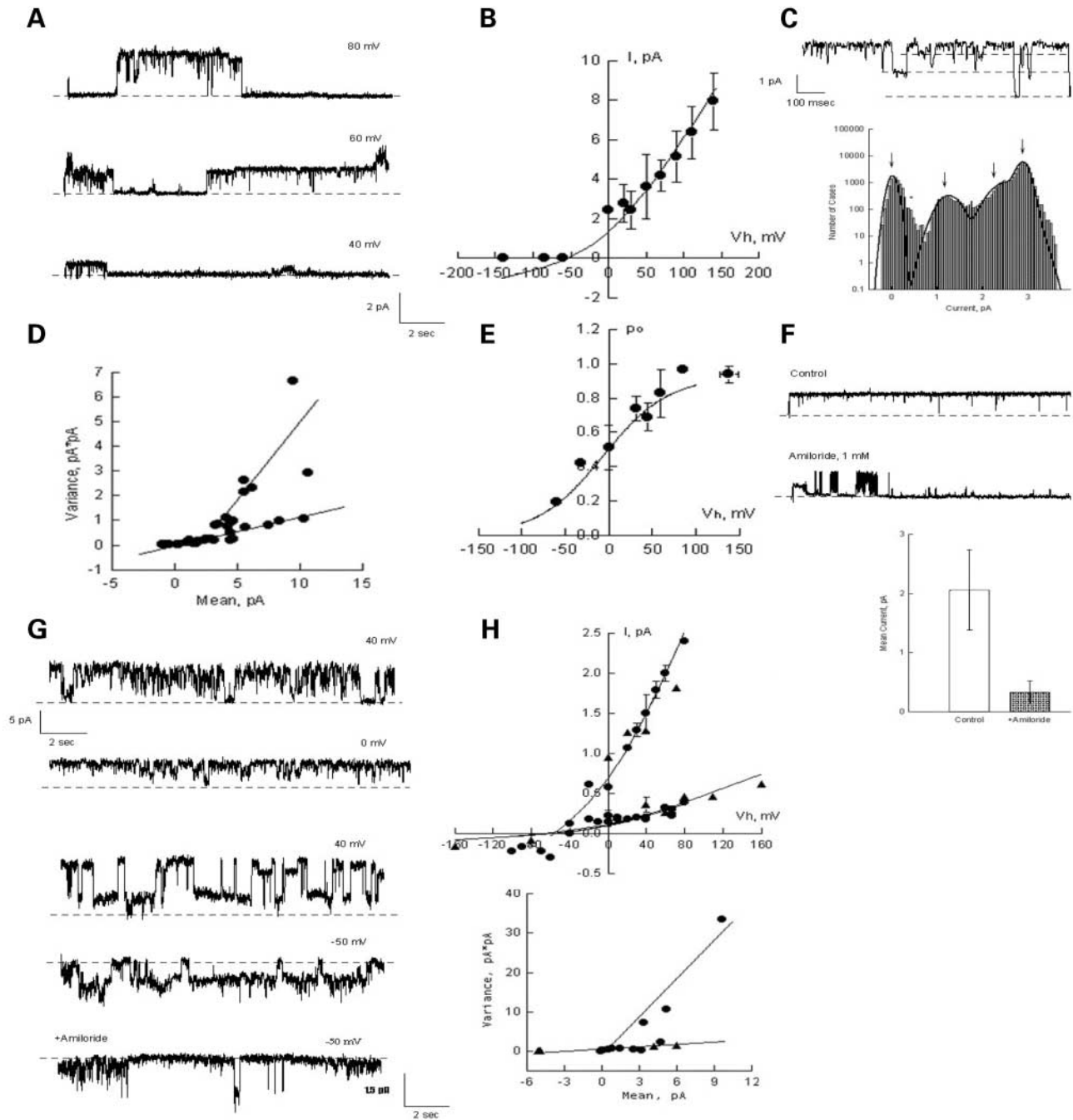


**Figure 2.** Functional characterization of *in vitro* translated ML1. WT- and mutant *in vitro* transcribed/translated ML1 constructs were incorporated into liposomes and studied by reconstitution in a lipid bilayer system. (A) Representative single channel currents of WT-ML1 in a  $K^+$  gradient. Data are representative of 25 experiments. Holding potentials are indicated on top of the tracings. (B) Current-to-voltage relationship of most frequent single channel conductance in asymmetrical  $K^+$  (filled circles,  $n = 3$ ). Solid line indicates GHK fitting of experimental data. The chord conductance was 46 pS. The reversal potential indicated a high cation/anion perm-selectivity ratio. (C) Subconductance states of WT-ML1 single channel currents are shown as dashed lines. Bottom: all-point histogram identifying closed, open and substates levels (arrows). (D) Mean versus variance analysis obtained from single channel currents (averaged 12.5 s) versus standard deviation squared from tracings at 40 mV. Slopes indicate prototypical single channel conductances. (E) Boltzmann distribution of open probability ( $p_o$ ) as a function of the holding potential ( $V_h$ ). Data (filled circles) are the mean  $\pm$  SEM of 4–7 experiments. Solid line indicates best fitting of data to a Boltzmann equation. (F) Effect of amiloride (1 mM) on the single-currents of *in vitro* translated WT-ML1 ( $n = 7$ ). Bottom: bar graph showing 84% decrease ( $P < 0.05$ ,  $n = 7$ ) in mean current after addition of amiloride. (G) Spontaneous single channel currents of both,  $\Delta F408$ - (top two tracings) and V446L- (bottom three tracings) mutant-ML1. Holding potentials are indicated on top of the tracings. Data are representative of 29 and six experiments, respectively. Tracings in V446L-ML1 were obtained in asymmetrical  $K^+/Na^+$  (135 mM, respectively). Currents were highly symmetrical, and inhibited by amiloride (1 mM,  $n = 3$ , bottom tracing). (H) Top: current-to-voltage relationships for the  $\Delta F408$ - (circles,  $n = 5$ ) and V446L- (triangles,  $n = 3$ ) ML1 channels. Low conductance single channel currents were most frequent, but higher conductance states were also observed for both mutant proteins. Bottom: mean versus variance analysis of V446L (triangles) and  $\Delta F408$  (circles) ML1 unmasked the most common smallest single channel conductance, which was similar for both mutants. Data were obtained at 40 mV.

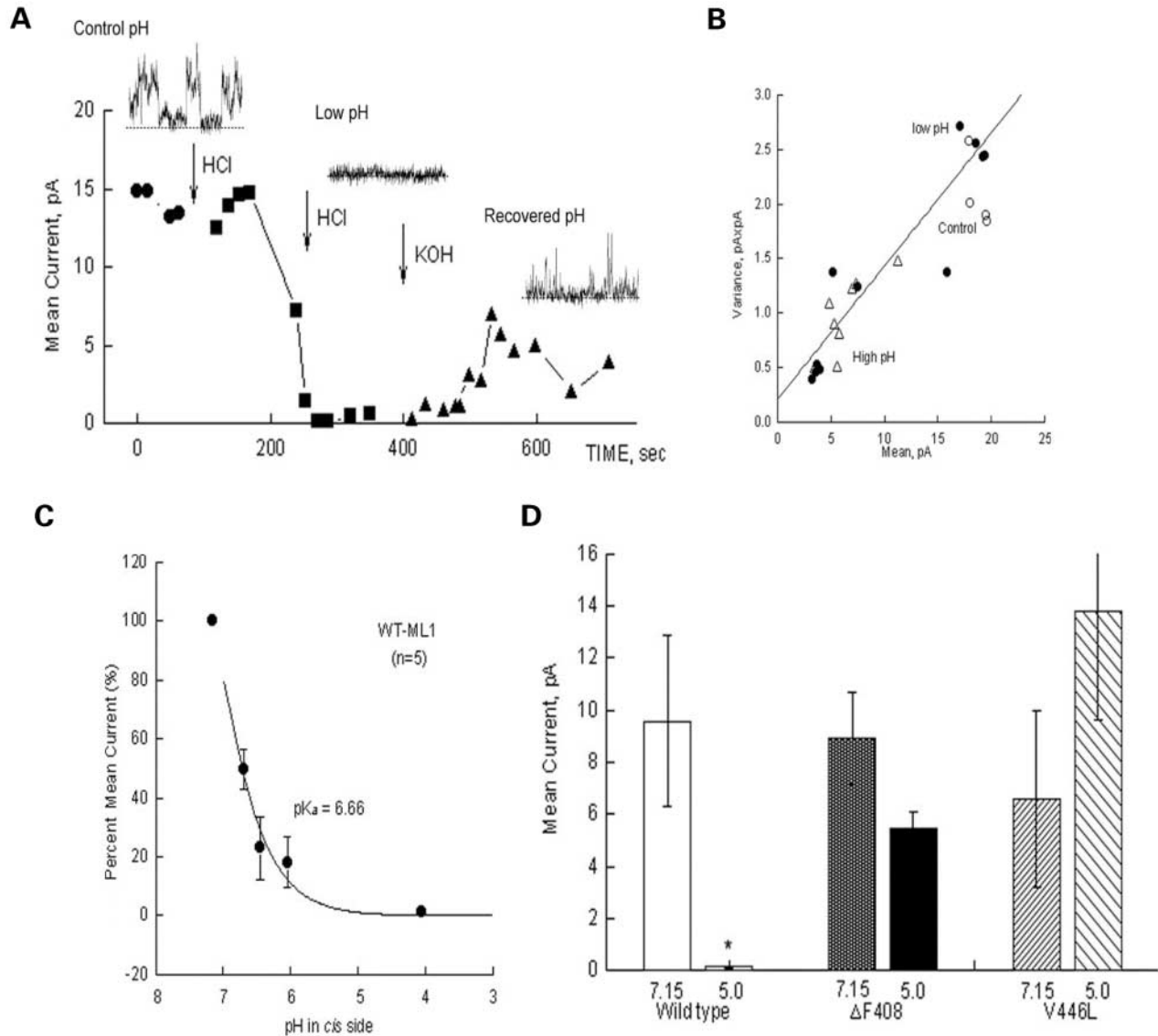


**Figure 3.** Effect of pH on ML1 channel currents. (A) WT-ML1 single channel currents were modulated by changes in  $pH_{cis}$ . Mean currents are shown before (circles), after addition of HCl (arrows, squares) and further addition of KOH (arrow, triangles). Representative tracings are shown on top. Data are representative of three experiments. (B) Mean versus variance analysis of single channel currents indicates that pH changes do not affect the ML1 single channel conductance,  $n = 5$ . (C) Effect of  $pH_{cis}$  on mean currents ( $I/I_{cr}$  ratio). Experimental data (filled circles) were fitted with a Henderson-Hasselbach type equation. The  $pK_a$  was 6.66. Data are the mean  $\pm$  SEM,  $n = 5$ . (D) Mean currents for WT-,  $\Delta F408$ - and V446L-mutated ML1 at normal (7.15) and low pH (5.0). Low pH (asterisk,  $P < 0.001$ ) reduced WT-, but not  $\Delta F408$  (lower) or V446L (higher) channel activity, which were not statistically different from respective controls. Data are the mean  $\pm$  SEM for 3–7 experiments for each protein.

ML1 in MLIV patients results in membrane abnormalities most pronounced in certain secretory epithelial cells (30). In MLIV patient fibroblasts, high uptake and slow lipid degradation (6), and/or lipid sorting abnormalities (29) have also been reported. Thus, ML1 function may be associated with vesicle trafficking. This would be relevant for proper vesicle trafficking and release during gastric secretion in stomach parietal cells. ML1 may also play a role in lipid containing vesicle trafficking associated to myelin formation and maintenance (31); thus, likely explaining brain abnormalities in MLIV patients (3). ML1 function may help stabilize membrane protein complexes, which in its absence deteriorate and change recycling through

the endosomal system. Loss-of-function mutations of the *MCOLN1* gene homolog in the *C. elegans* (CUP-5), for example, lead to endocytic defects, the formation of large lysosomal vacuoles and increased apoptosis (25,26). The recently described mouse mucolipin-3 (ML3) localizes to cytoplasmic compartments of hair cells and stereocilia (32). ML3 expression may play a critical role in vesicular structures and melanosome transport (33). Although ML3 function is still unknown, skin pigmentation abnormalities are associated with defects in vesicle function and dysfunctional trafficking of late-stage melanosomes (34–37). In mice, ML3 deficiency causes deafness, a phenomenon that

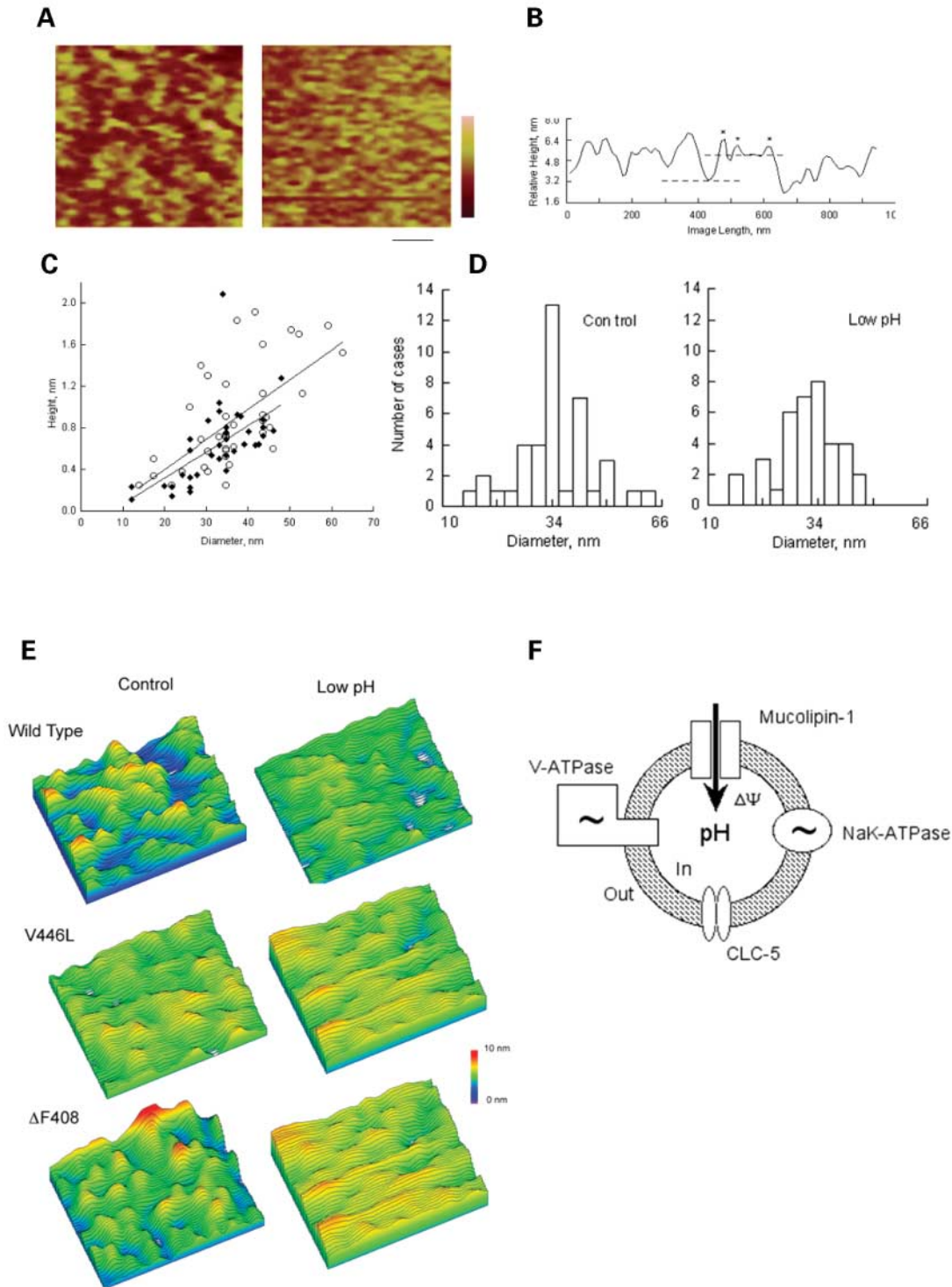


**Figure 4.** Atomic force imaging of ML1 complexes. *In vitro* translated WT-ML1 containing proteoliposomes were flattened and imaged onto freshly cleaved mica in solution, with tapping mode AFM. (A) WT-ML1 complexes aggregated at normal pH (left). Low pH reduced the size of the complexes (right). Horizontal bar is 200 nm and vertical bar is 10 nm. Data are representative of three experiments. (B) Scan line in A. Distance between dashed lines is the height of the lipid layers. Asterisks indicate individual ML1 complexes. (C) Diameter versus height correlation for normal ( $n=40$ , open circles) and low pH ( $n=37$ , filled triangles). Controls show a larger average diameter. (D) Histogram distribution for individual ML1 complex diameters in normal (left,  $n=40$ ) and low pH (right,  $n=37$ ). A reduction of molecular size is shown at low pH. Data were processed with Image SXM v. 1.62 (Steve Barrett, Public Domain, 1999),  $n=3$ . (E) WT-ML1 complexes disassembled at low pH (right). Low pH ML1 channel disassembly was not as evident (right) in either V446L-ML1 (center) or  $\Delta F408$ -ML1 (bottom). Areas are  $140 \text{ nm} \times 200 \text{ nm}$ . Data were processed as in Fig. 4C,  $n=2-3$  samples for each group. (F) Hypothetical model of ML1 control of endosome/lysosomal function. Cation channel function of normal ML1 (arrow) controls vesicular membrane potential ( $\Delta\Psi$ ) by switching off at low pH, which provides the driving force for  $\text{H}^+$  accumulation driven by other transporters. The inability of mutated ML1 to 'shut off' at low pH is in agreement with dissipation of the vesicular  $\text{H}^+$  gradient. Thus, ML1 function may modify vesicle trafficking and function by controlling intravesicular pH (54).

has been hypothesized to ML-related Trp-type channel activity (32).

The present study indicates that ML1-containing endosomal membranes display distinct channel activity not observed in the *MCOLN1*<sup>-/-</sup> cells. The ML1 constructs used in our endosomal experiments were labeled with, and recognized by, a FLAG-tagged to the carboxy-terminal end of the protein and anti-FLAG antibodies (see Materials and Methods, Stratagene), respectively. The FLAG-tagging localized mainly in intracellular vesicles, suggesting the presence and likely role of the tagged ML1 in the endosome/lysosome vesicular system. This interpretation, although consistent with the theorized role of ML proteins in cell function, has to be carefully evaluated in experiments where artificially tagged proteins are expressed in cells. Trp channels would appear to localize to the expected membrane domain only when expressed as part of a 'native complex' (38,39). Lysosome-containing dense endosomal membranes were used in this study, because this fraction contained the majority of the FLAG-tagged protein. Whether this applies to the endogenous channel will require further experimentation and yet unavailable anti-ML1 antibodies.

The data provide functional support to the idea that ML1 channel indeed is a Trp family member (40,41), with which it shares partial homology and membrane topology (10). In particular, human ML1 shares similarity with polycystin-2, another Trp channel (10). Trp channels are quintessentially related to Ca<sup>2+</sup> entry steps and capacitative responses (42) in a number of sensory transduction responses (43–45). Polycystin-2 has recently been implicated in mechano-transduction in renal epithelial cells (46). Further, polycystin-2 has been localized to both cell membranes and intracellular compartments, such as the endoplasmic reticulum (38,47), where it may help release intracellular Ca<sup>2+</sup> (47). In our studies, endosomal vesicles containing WT- and ΔF408 ML1 showed channel activity not seen in either naïve (*MCOLN1*<sup>-/-</sup>) cells or cells expressing D362Y ML1. This mutation localizes to TM3 domain in ML1 (2). This region is potentially important in the sensor domain of Trp and voltage gated K<sup>+</sup> channels (48). Interestingly, the ADPKD causing mutation D511V in polycystin-2, which localizes to TM3, was found devoid of channel activity (47). Thus, when present in vesicular compartments, ML1 may regulate vesicular membrane potential, the process of acidification associated with normal vesicular function, and/or Ca<sup>2+</sup> transport, into intracellular organelles. Cation transport signaling events trigger vesicle trafficking and fusion (49), and Ca<sup>2+</sup> release-coupled K<sup>+</sup> transport across Ca<sup>2+</sup> storage organelles such as the endoplasmic reticulum (49,50). To date, little is known about the molecular identity of cation transport electrodiffusional pathways in the endosome/lysosomal pathways. The presence of ML1 in endosomes, combined with its ability to allow non-selective cation movement, and its sensitivity to pH, provide the first indication for a functional mechanism implicated in vesicular regulation. WT-, but not mutant-ML1 was inhibited at low cellular pH. This suggests a pH-sensitive regulatory mechanism for vesicular function, in agreement with previous evidence indicating that MLIV displays abnormal lysosomal pH (27). A dysregulated (or absent) ML1 channel would likely cause this abnormality. Nevertheless, the absence of pH inhibition by mutant-ML1, may imply higher, instead of lower, channel activity. Thus,

further studies will be required to assess whether compensatory mechanisms are at work which indicate the complementary role of yet unknown transport mechanisms in the absence of a functional ML1.

Most intracellular organelles along the endocytic and secretory pathways, as well as lysosomes, have characteristic acidic intravesicular pH suited to their biological function. The establishment of a pH gradient within the endosomes is a central feature of the endocytic trafficking pathway (51) (Fig. 4F). In this process, V-type ATPases elicit an uphill H<sup>+</sup> electrochemical gradient, which is accompanied by Cl<sup>-</sup> counterion movement by ClC-type channels and the consequent intravesicular acidification (Fig. 4F). This gradient is maintained and controlled by cation transport by various proteins, including the Na<sup>+</sup>, K<sup>+</sup>-ATPase and cation-selective channels. Endosomal vesicles and Golgi complexes are permeable to counter ions such as Cl<sup>-</sup> and K<sup>+</sup>, which can also affect vesicular pH by altering the vesicular membrane potential (52,53). Cation channel ML1 function as shown in this report, may be considered relevant to vesicular acidification (54,55). A feedback mechanism may thus be postulated for ML1 function to help control intravesicular pH (54) (Fig. 4F) and intravesicular resting potential. This latter mechanism is a main contributor to the driving force for lowering pH in intracellular vesicles (51,55,56).

In summary, the data in this report provide the first molecular evidence for a dysfunctional ML1 cation channel, as a potential contributor to MLIV disease. The pH regulation of ML1 may be central to its normal function, in particular when the channel is located in vesicular compartments. In this context, the data places new emphasis in the regulatory role of cation-selective channels as a novel control mechanism in vesicular transport. ML1 other locations and role(s) in cell function still await further experimentation.

## MATERIALS AND METHODS

### Cells lacking and expressing the MCOLN1 gene product

*MCOLN1*<sup>-/-</sup> fibroblasts were originally obtained from DMNB at NINDS. The WT *MCOLN1* gene was transiently expressed in *MCOLN1*<sup>-/-</sup> cells from patients either homozygous to the 6.4 kb deletion in *MCOLN1* (g.511–6944del) or heterozygous for that mutation and the splice mutation (g.5534A-G; *MCOLN1* genomic GenBank accession number AF287270). Cells were grown in EMEM + 10% fetal bovine serum and transfected with either WT or mutated mucolipin constructs in pSPORT1 plasmid (Life Technologies) using Fugene transfection reagent (Roche Appl. Sci., Indianapolis, IN). Mutations used were c.1209G-T (D362Y), c.1346–1348delCTT (ΔF408), c.1461G-T (V466L) (*MCOLN1* cDNA GenBank accession number AF287269). All constructs contained a carboxy-terminus FLAG, consisting of the tagged sequence DYKDDDDK (Stratagene, CA).

### Dense membrane preparation

Endosome-containing, dense membrane fractions were prepared by differential centrifugation. Briefly, 72 h after

transfection, cells were washed with PBS, harvested by scraping in Tris EDTA pH 7.4 containing Complete Protease Inhibitor mixture (Roche) and spun down. Pellets were homogenized in the same solution, and spun down for 10 min at 1000g, at 4°C. The supernatant was spun for 15 min at 14 000g. The dense membrane-containing pellet was suspended in water and frozen. In this fraction, lysosomes and late endosomes were preferentially obtained, with some mitochondria as confirmed by enzyme markers. Late endosomal and lysosomal enrichment was confirmed by succinic-reductase detection, mitochondria with  $\beta$ -hexosaminidase. Golgi apparatus and nucleus enzymes were also detected. Enrichment of the ML1 constructs in the dense membrane fraction was confirmed by western blot with anti-FLAG mouse monoclonal antibodies (Stratagene, CA). The majority of the protein content in this preparation, which comprised ~10% of cellular protein, consisted of late-endosomal/lysosomal material. There was only some Golgi and mitochondrial contamination in this preparation, based on marker analysis, which did not contain nuclei on microscopic examination.

#### ***In vitro* transcription/translation of Mucolipin-1**

*In vitro* translation of WT-ML1 and two mutants, V446L-ML1 and  $\Delta$ F408-ML1, was performed with a Promega kit (Madison, WI, USA) as previously described (57). Briefly, the cDNAs were subcloned in pSV-SPORT1 expression vector to generate specific constructs. The cDNAs within the vector were *in vitro* transcribed and translated with the TnT-T7-coupled reticulocyte system (Promega, WI).

#### **Mucolipin-1 proteoliposome preparations**

ML1 containing proteoliposomes were prepared with a lipid mixture of phosphatidyl ethanolamine (75%) and phosphatidyl serine (25%) (Avanti Polar Lipids, Birmingham, AL). The phospholipid mixture was sonicated with a solution containing 150 mM NaCl, 0.1 mM EDTA, 20 mM HEPES, pH 7.2 and 25 mM Na<sup>+</sup>-cholate. *In vitro* translated ML1 was added to the Na<sup>+</sup>-cholate solution (0.55 mM) and the phospholipid mixture (10 mg/ml). The mixture was dialyzed for three days in 150 mM NaCl, 0.1 mM EDTA, 20 mM HEPES, pH 7.2, with three buffer changes to eliminate residual detergent and obtain the proteoliposomes used in the functional assays. Samples were separated by 4–12% SDS–PAGE and stained with Simply Blue<sup>TM</sup> Safe Stain (Invitrogen, CA).

#### **Solutions and changes in pH**

The lipid bilayer solution was prepared as follows. A buffer solution was prepared with 10 mM MOPS and 10 mM MES, and was adjusted with KOH to reach pH 7.4. This solution had a final K<sup>+</sup> concentration of 15 mM at room temperature. The solution also contained 10–15  $\mu$ M CaCl<sub>2</sub>. To create a KCl chemical gradient, the *cis* side of the chamber was added KCl to a final concentration of 150 mM. Whenever indicated, the *trans* compartment was added KCl, NaCl or CaCl<sub>2</sub> to determine the cation permeability ratio (perm-selectivity) in the presence of two different ion salts in either compartment of the reconstitution chamber. Changes in pH were conducted as

recently reported (19) by addition of either HCl or KOH to either side of the chamber. Final pH was calibrated with a pH mini-electrode.

#### **Electrical recordings and data analysis**

Ion channel reconstitution was conducted as previously described (19,58). Briefly, lipid bilayers were formed with a mixture of synthetic phospholipids. The phospholipid composition of the lipid bilayers was 1-palmitoyl-2-oleyl-sn-glycero-3-phosphatidylethanolamine: 1-palmitoyl-2-oleyl-sn-glycero-3-phosphatidylcholine (7:3, v/v, Avanti Polar Lipids, Alabaster, AL) in n-decane (Sigma) to final concentrations of 14 and 6 mM, respectively (19,58). All phospholipids used were 1-palmitoyl-2-oleoyl-based, the polar head group being choline (POPC) and ethanolamine (POPE). The lipid solution (~20–25 mg/ml) was used to 'paint', with a thin glass rod, the opening (250  $\mu$ m diameter) of the polystyrene cuvette (CP13-150). The hole separates the two compartments (*cis* and *trans*) of the reconstitution chamber (model BCH-13, Warner Instruments Corp.). The cuvette was inserted into a polyvinyl-chloride holder, thus defining two aqueous compartments of volumes 800 and 1600  $\mu$ l, respectively, and separated by a planar lipid film. Both sides of the lipid bilayer were bathed with a MOPS/MES-KOH buffered solution as described below. Experiments were initiated by bathing the *trans* side of the bilayer with this solution after further addition of KCl to the *cis* side of the chamber to generate a trans-bilayer osmotic gradient that promotes vesicle-planar bilayer membrane fusion. Holding potentials ( $V_h$ ) were applied, and electrical signals were recorded using a patch-clamp amplifier as previously reported (19,58). The patch-clamp amplifier contained a 10 Gohm head-stage for lipid bilayers (PC-510A Warner Instrument Corp., Hamden, CT). Output (voltage) signals were low-pass filtered at 1 kHz (–3 dB) with an eight pole Bessel type filter (Frequency Devices, Haverhill, MA). Whenever indicated, electrical recordings from single channel activity (current tracings) were further filtered (see Results) for display purposes only. PClamp 5.5.1 (Axon Instruments, Foster City, CA) was used for data analysis and Sigmaplot Version 2.0 (Jandel Scientific, Corte Madera, CA) for statistical analysis and graphics. Single channel conductances were calculated from best-fitted current-to-voltage data with the Goldman–Hodgkin–Katz (GHK) equation as reported (19,58). Open probability ( $p_o$ ) was obtained from exponential fitting of dwell-time histograms, and fitted to a Boltzmann equation (19,58). Statistical significance, accepted at  $P < 0.05$ , was obtained by paired 't' test. Data were expressed as the mean  $\pm$  SEM. 'n' represents the number of experiments analyzed. Mean versus variance (noise) analysis was conducted as previously reported (15,16).

#### **Atomic force microscopy**

ML1 protein complexes were imaged with a Model 3000 atomic force microscope (AFM) attached to a Nanoscope IIIa controller (Digital Intr., St Barbara, CA) as recently reported for another channel protein (24). Samples were scanned with oxide-sharpened silicon-nitride tips (DNP-S, Digital Instr.). *In vitro* translated ML1-containing proteoliposomes used for the lipid-bilayer reconstitution studies were used for AFM

imaging studies. Proteoliposomes were flattened in saline solution, containing 0.2 mM CaCl<sub>2</sub>, 0.2 mM MgATP, 0.2 mM β-mercaptoethanol and 2 mM Tris-HCl, pH 7.15–7.25, onto freshly cleaved mica disks. Samples were incubated for either ~30 min at 37°C or 15 min at room temperature, with similar results. Small volumes (~2 μl) of HCl (1 N) were added to change pH.

## ACKNOWLEDGEMENTS

M.K.R. was supported by NIH Training Grant T32DK07540C15.

## REFERENCES

- Berman, E.R., Livni, N., Shapira, E., Merin, S. and Levij, I.S. (1974) Congenital corneal clouding with abnormal systemic storage bodies: a new variant of mucopolipidosis. *J. Pediatr.*, **84**, 519–526.
- Altarescu, G., Sun, M., Moore, D., Smith, J., Wiggs, E., Solomon, B., Patronas, N., Frei, K., Gupta, S., Kaneski, C. *et al.* (2002) The neurogenetics of mucopolipidosis type IV. *Neurology*, **59**, 306–313.
- Frei, K.P., Patronas, N.J., Crutchfield, K.E., Altarescu, G. and Schiffmann, R. (1998) Mucopolipidosis type IV: characteristic MRI findings. *Neurology*, **51**, 565–569.
- Goldin, E., Blanchette-Mackie, E.J., Dwyer, N.K., Pentchev, P.G. and Brady, R.O. (1995) Cultured skin fibroblasts derived from patients with mucopolipidosis 4 are auto-fluorescent. *Pediatr. Res.*, **37**, 687–669.
- Smith, J.A., Chan, C.C., Goldin, E. and Schiffmann, R. (2002) Noninvasive diagnosis and ophthalmic features of mucopolipidosis type IV. *Ophthalmology*, **109**, 588–594.
- Hammel, I. and Alroy, J. (1995) The effect of lysosomal storage diseases on secretory cells: an ultrastructural study of pancreas as an example. *J. Submicrosc. Cytol. Pathol.*, **27**, 143–160.
- Agnew, B.J., Duman, J.G., Watson, C.L., Coling, D.E. and Forte, J.G. (1999) Cytological transformations associated with parietal cell stimulation: critical steps in the activation cascade. *J. Cell Sci.*, **112**, 2639–2646.
- Schiffmann, R., Dwyer, N.K., Lubensky, I.A., Tsokos, M., Sutliff, V.E., Latimer, J.S., Frei, K.P., Brady, R.O., Barton, N.W., Blanchette-Mackie, E.J. *et al.* (1998) Constitutive achlorhydria in mucopolipidosis type IV. *Proc. Natl Acad. Sci. USA*, **95**, 1207–1212.
- Bassi, M.T., Manzoni, M., Monti, E., Pizzo, M.T., Ballabio, A. and Borsani, G. (2000) Cloning of the gene encoding a novel integral membrane protein, mucolipidin- and identification of the two major founder mutations causing mucopolipidosis type IV. *Am. J. Hum. Genet.*, **67**, 1110–1120.
- Sun, M., Goldin, E., Stahl, S., Falardeau, J.L., Kennedy, J.C., Aciermo, J.S.J., Bove, C., Kaneski, C.R., Nagle, J., Bromley, M.C. *et al.* (2000) Mucopolipidosis type IV is caused by mutations in a gene encoding a novel transient receptor potential channel. *Hum. Mol. Genet.*, **9**, 2471–2478.
- Bach, G. (2001) Mucopolipidosis type IV. Minireview. *Mol. Genet. Metab.*, **73**, 197–203.
- Bargal, R., Avidan, N., Ben-Asher, E., Olender, Z., Zeigler, M., Frumkin, A., Raas-Rothschild, A., Glusman, G., Lancet, D. and Bach, G. (2000) Identification of the gene causing mucopolipidosis type IV. *Nat. Genet.*, **26**, 118–123.
- Slaugenhaupt, S.A., Aciermo, J.S.J., Helbing, L.A., Bove, C., Goldin, E., Bach, G., Schiffmann, R. and Gusella, J.F. (1999) Mapping of the mucopolipidosis type IV gene to chromosome 19p and definition of founder haplotypes. *Am. J. Hum. Genet.*, **65**, 773–778.
- LaPlante, J.M., Falardeau, J., Sun, M., Kanazirska, M., Brown, E.M., Slaugenhaupt, S.A. and Vassilev, P.M. (2002) Identification and characterization of the single channel function of human mucolipin-1 implicated in mucopolipidosis type IV, a disorder affecting the lysosomal pathway. *FEBS Lett.*, **532**, 183–187.
- Kolesnikov, S.S. and Margolskee, R.F. (1998) Extracellular K<sup>+</sup> activates a K<sup>+</sup>- and H<sup>+</sup>-permeable conductance in frog taste receptor cells. *J. Physiol.*, **507**, 415–432.
- Patlak, J.B. (1988) Sodium channel subconductance levels measured with a new variance-mean analysis. *J. Gen. Physiol.*, **92**, 413–430.
- Hille, B. (1992) *Ionic Channels of Excitable Membranes*. Sinauer Associates Inc: Sunderland, MA.
- Sigworth, F.J. (1984) Non-stationary of membrane currents. In Eisenberg, R.S., Frank, M. and Stevens, C. (eds) *Membrane, Channels and Noise*, Plenum Publishing Corp.: New York, pp. 21–48.
- González-Perrett, S., Batelli, M., Kim, K., Essafi, M., Timpanaro, G., Montalbetti, N., Reisin, I.L., Arnaout, M.A. and Cantiello, H.F. (2002) Voltage dependence and pH regulation of human polycystin-2 mediated cation channel activity. *J. Biol. Chem.*, **277**, 24959–24966.
- Clay, J.R. and Kuzirian, A.M. (2002) Trafficking of axonal K<sup>+</sup> channels: potential role of Hsc70. *J. Neurosci. Res.*, **67**, 745–752.
- Clay, J.R. and Kuzirian, A.M. (2000) Localization of voltage-gated K<sup>+</sup> channels in squid giant axons. *J. Neurobiol.*, **45**, 172–184.
- Shuai, J.W. and Jung, P. (2003) Optimal ion channel clustering for intracellular calcium signaling. *Proc. Natl Acad. Sci. USA*, **100**, 506–510.
- Bray, D., Levin, M.D. and Morton-Firth, C.J. (1998) Receptor clustering as a cellular mechanism to control sensitivity. *Nature*, **393**, 85–88.
- Chasan, B., Geisse, N.A., Pedatella, K., Wooster, D.G., Teintze, M., Carattino, M.D., Goldmann, W.H. and Cantiello, H.F. (2002) Evidence for direct interaction between actin and the cystic fibrosis transmembrane conductance regulator. *Eur. Biophys. J.*, **30**, 617–624.
- Fares, H. and Greenwald, I. (2001) Regulation of endocytosis by CUP-5, the *Caenorhabditis elegans* mucolipin-1 homolog. *Nat. Genet.*, **28**, 64–68.
- Hersh, B., Hartweg, E. and Horvitz, H. (2002) The *Caenorhabditis elegans* mucolipin-like gene cup-5 is essential for viability and regulates lysosomes in multiple cell types. *Proc. Natl Acad. Sci. USA*, **99**, 4355–4360.
- Bach, G., Chen, C.S. and Pagano, R.E. (1999) Elevated lysosomal pH in Mucopolipidosis type IV cells. *Clin. Chim. Acta*, **280**, 173–179.
- Bargal, R. and Bach, G. (1997) Mucopolipidosis type IV: abnormal transport of lipids to lysosomes. *J. Inherit. Metab. Dis.*, **20**, 625–632.
- Chen, C.S., Bach, G. and Pagano, R.E. (1998) Abnormal transport along the lysosomal pathway in Mucopolipidosis type IV disease. *Proc. Natl Acad. Sci. USA*, **95**, 6373–6378.
- Lubensky, I.A., Schiffmann, R., Goldin, E. and Tsokos, M. (1999) Lysosomal inclusions in gastric parietal cells in mucopolipidosis type IV: a novel cause of achlorhydria and hypergastrinemia. *Am. J. Surg. Pathol.*, **23**, 1527–1531.
- Larocca, J.N. and Rodriguez-Gabin, A.G. (2002) Myelin biogenesis: vesicle transport in oligodendrocytes. *Neurochem. Res.*, **27**, 1313–1329.
- Di Palma, F., Belyantseva, I., Kim, H.J., Vogt, T.F., Kachar, B. and Noben-Trauth, K. (2002) Mutations in Mcoln3 associated with deafness and pigmentation defects in varitint-waddler (Va) mice. *Proc. Natl Acad. Sci. USA*, **99**, 14994–14999.
- Kachar, B., Battaglia, A. and Fex, J. (1997) Compartmentalized vesicular traffic around the hair cell cuticular plate. *Hear. Res.*, **107**, 102–112.
- Lofthus, S.K., Larson, D.M., Baxter, L.L., Antonellis, A., Chen, Y., Wu, X., Jiang, Y., Bittner, M., Hammer, III, J.A. and Pavan, W.J. (2002) Mutation of melanosome protein RAB38 in chocolate mice. *Proc. Natl Acad. Sci. USA*, **99**, 4471–4476.
- Matesic, L.E., Yip, R., Reuss, A.E., Swing, D.A., O'Sullivan, T.N., Fletcher, C.F., Copeland, N.G. and Jenkins, N.A. (2001) Mutations in Mlph, encoding a member of the Rab effector family, cause the melanosome transport defects observed in leaden mice. *Proc. Natl Acad. Sci. USA*, **98**, 10238–10243.
- Wilson, S.M., Yip, R., Swing, D.A., O'Sullivan, T.N., Zhang, Y., Novak, E.K., Swank, R.T., Russell, L.B., Copeland, N.G. and Jenkins, N.A. (2000) A mutation in Rab27a causes the vesicle transport defects observed in ash mice. *Proc. Natl Acad. Sci. USA*, **97**, 7933–7938.
- Wu, X.S., Rao, K., Zhang, H., Wang, F., Sellers, J.R., Matesic, L.E., Copeland, N.G., Jenkins, N.A. and Hammer, J.A. (2002) Identification of an organelle receptor for myosin-Va. *Nat. Cell Biol.*, **4**, 271–278.
- Luo, Y., Vassilev, P.M., Li, X., Kawanabe, Y. and Zhou, J. (2003) Native polycystin 2 functions as a plasma membrane Ca<sup>2+</sup>-permeable cation channel in renal epithelia. *Mol. Cell Biol.*, **23**, 2600–2607.
- Xu, X.Z., Li, H.S., Guggino, W.B. and Montell, C. (1997) Coassembly of TRP and TRPL produces a distinct store-operated conductance. *Cell*, **89**, 1155–1164.
- Montell, C., Birnbaumer, L. and Flockerzi, V. (2002) The TRP channels, a remarkably functional family. *Cell*, **108**, 595–598.
- Montell, C., Birnbaumer, L., Flockerzi, V., Bindels, R.J., Bruford, E.A., Caterina, M.J., Clapham, D.E., Harteneck, C., Heller, S., Julius, D. *et al.*

- (2002) A unified nomenclature for the superfamily of TRP cation channels. *Mol. Cell*, **9**, 229–231.
42. Birnbaumer, L., Zhu, X., Jiang, M., Boulay, G., Peyton, M., Vannier, B., Brown, D., Platano, D., Sadeghi, H., Stefani, E. *et al.* (1996) On the molecular basis and regulation of cellular capacitative calcium entry: roles for Trp proteins. *Proc. Natl Acad. Sci. USA*, **93**, 15195–15202.
  43. Goodman, M.B. and Schwarz, E.M. (2003) Transducing touch in *Caenorhabditis elegans*. *Annu. Rev. Physiol.*, **65**, 429–452.
  44. Montell, C. (2001) Physiology, phylogeny, and functions of the TRP superfamily of cation channels. *Sci. STKE*, **90**, RE1.
  45. Voets, T. and Nilius, B. (2003) TRPs Make Sense. *J. Membr. Biol.*, **192**, 1–8.
  46. Nauli, S.M., Alenghat, F.J., Luo, Y., Williams, E., Vassilev, P., Li, X., Elia, A.E.H., Lu, W., Brown, E.M., Quinn, S.J. *et al.* (2003) Polycystins 1 and 2 mediate mechanosensation in the primary cilium of kidney cells. *Nature Genet.*, **33**, 129–137.
  47. Koulen, P., Cai, Y., Geng, L., Maeda, Y., Nishimura, S., Witzgall, R., Ehrlich, B.E. and Somlo, S. (2002) Polycystin-2 is an intracellular calcium release channel. *Nat. Cell Biol.*, **4**, 191–197.
  48. Jiang, Y., Ruta, V., Chen, J., Lee, A. and MacKinnon, R. (2003) The principle of gating charge movement in a voltage-dependent  $K^+$  channel. *Nature*, **423**, 42–48.
  49. Nguyen, T., Chin, W.C. and Verdugo, P. (1998) Role of  $Ca^{2+}/K^+$  ion exchange in intracellular storage and release of  $Ca^{2+}$ . *Nature*, **395**, 908–912.
  50. O'Rourke, F., Soons, K., Flaumenhaft, R., Watras, J., Baio-Larue, C., Matthews, E. and Feinstein, M.B. (1994)  $Ca^{2+}$  release by inositol 1,4,5-trisphosphate is blocked by the  $K^+$ -channel blockers apamin and tetrapentylammonium ion, and a monoclonal antibody to a 63 kDa membrane protein: reversal of blockade by  $K^+$  ionophores nigericin and valinomycin and purification of the 63 kDa antibody-binding protein. *Biochem. J.*, **300**, 673–683.
  51. Marshansky, V., Ausiello, D.A. and Brown, D. (2002) Physiological importance of endosomal acidification: potential role in proximal tubulopathies. *Curr. Opin. Nephrol. Hypertens.*, **11**, 527–537.
  52. Schapiro, F. and Grinstein, S. (2000) Determinants of the pH of the Golgi complex. *J. Biol. Chem.*, **275**, 21025–21032.
  53. Van Dyke, R.W. and Belcher, J.D. (1994) Acidification of three types of liver endocytic vesicles: similarities and differences. *Am. J. Physiol.*, **266**, C81–C94.
  54. Grabe, M. and Oster, G. (2001) Regulation of organelle acidity. *J. Gen. Physiol.*, **117**, 329–343.
  55. Rybak, S.L., Lanni, F. and Murphy, R.F. (1997) Theoretical considerations on the role of membrane potential in the regulation of endosomal pH. *Biophys. J.*, **73**, 674–687.
  56. Marshansky, V. and Vinay, P. (1996) Proton gradient formation in early endosomes from proximal tubules. *Biochem. Biophys. Acta*, **1284**, 171–180.
  57. Xu, G.M., González-Perrett, S., Essafi, M., Timpanaro, G.A., Montalbetti, N., Arnaout, M.A. and Cantiello, H.F. (2003) Polycystin-1 activates and stabilizes the polycystin-2 channel. *J. Biol. Chem.*, **278**, 1457–1462.
  58. González-Perrett, S., Kim, K., Ibarra, C., Damiano, A.E., Zotta, E., Batelli, M., Harris, P.C., Reisin, I.L., Arnaout, M.A. and Cantiello, H.F. (2001) Polycystin-2, the protein mutated in autosomal dominant polycystic kidney disease (ADPKD), is a  $Ca^{2+}$ -permeable nonselective cation channel. *Proc. Natl Acad. Sci. USA*, **98**, 1182–1187.